Research Article | Vol. 28, No. 9 / 27 April 2020 / Optics Express 13907
Optics EXPRESS

Absorption-based polarization gratings

TAO ZHAN, JIANGHAO XIONG, GUANJUN TAN, AND SHIN-TSON WU*

College of Optics and Photonics, University of Central Florida, Orlando, FL 32816, USA
**swu@creol.ucf.edu*

Abstract: We demonstrate an absorption-based polarization grating made of dichroic dye-doped polymerizable liquid crystal. These gratings manifest a polarization-sensitive diffraction efficiency over the absorption band of the employed dye material, based on our theoretical analysis and experimental evidence. The spectral range can be easily tailored by varying the dye material. Since these gratings generate first-order diffracted beams with orthogonal circular polarizations, they can be utilized as key components in polarimetry systems. Meanwhile, due to their absorptive nature, these polarization gratings can function as LED-compatible polarization masks for photopatterning while fabricating various liquid crystal devices.

1. Introduction

The management and measurement of polarization are ubiquitously important in a plethora of optical systems including but not limited to displays, polarimetry, ellipsometry, remote sensing, and quantum computing. As a compact alternative to polarizing beam splitter, conventional Pancharatnam-Berry phase deflector (PBD) [1,2], which is a special type of polarization grating (PG) [3,4], has been extensively studied and developed during this decade due to its high diffraction efficiency and polarization sensitivity. The spatially varying anisotropy in PBDs can be achieved through patterning liquid crystals (LCs) [5] and LC polymers [6] or lithography-based nanofabrication [7]. Most of the conventional PBDs are retardation-based PGs that show 100% diffraction efficiency when the half-wave retardation condition is satisfied. Thus, such a PBD is also called diffractive waveplate [8]. Besides the retardation-based PGs, spatially varying anisotropic absorption also has the potential to enable polarization-sensitive gratings [3]. To distinguish this type of PGs from conventional ones, here we call them absorption-based polarization gratings (a-PGs).

In this paper, we demonstrate a-PGs formed with a dichroic dye and a polymerizable liquid crystal reactive mesogen (RM). In theory, this periodic anisotropic absorption profile manifests ~25% diffraction efficiency for a circularly polarized input light across the absorption band of the dye material. In this case, another 25% is directly transmitted as the zero-order leakage and maintains the original polarization state. Since a-PGs can separate orthogonal circular polarizations to distinct first-orders, they can be employed in polarimetry systems similar to conventional PBDs [6]. Also, photopatterning of LCs can also be simplified using a-PGs because they are naturally polarization masks that are compatible with broadband light sources, such as LEDs.

2. Paraxial analysis

The paraxial diffraction behavior of a-PGs can be derived analytically with Jones calculus as presented by Gori [3], where the a-PGs are theoretically proposed for polarimetry applications. Since the dichroic dye molecule orientation rotates 180° in one period, the direction of the in-plane transmission axis in a-PGs can be described by

$$\varphi = \frac{\pi x}{\Lambda}, \tag{1}$$

#392550 https://doi.org/10.1364/OE.392550
Journal © 2020 Received 10 Mar 2020; revised 14 Apr 2020; accepted 16 Apr 2020; published 22 Apr 2020

Optics EXPRESS

where φ is the orientation angle relative to the x axis (the periodic direction) and Λ denotes the grating period. For simplicity, the a-PG profile is modeled in a single period. The output local polarization direction associated with the dichroic dye orientation is illustrated in Fig. 1.

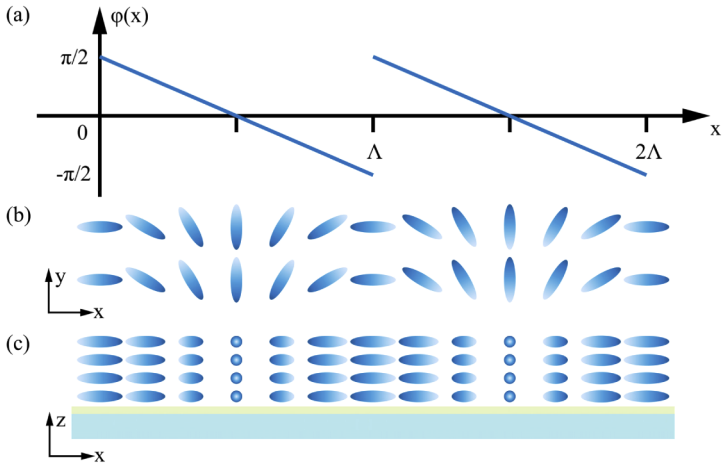

Fig. 1. (a) Local transmission direction followed by (b) front and (c) side view of the dichroic dye director orientations in absorption-based polarization gratings (a-PGs).

It is convenient to achieve this profile using dichroic-dye-doped RMs since they can be photo-aligned by a polarized light field [5] and then fixed after photopolymerization. Under paraxial approximation, the output electric field after the a-PG can be expressed by transforming the input field $\mathbf{E}_{in}$ with the local Jones matrix of the polarizer grating $\mathbf{T}(x)$. Based on these assumptions, the far-field electric field of diffracted order m can be expressed as follows:

$$\mathbf{D}_m = \frac{1}{\Lambda}\int_0^{\Lambda} \mathbf{T}(x)\mathbf{E}_{in}\exp(-i2\pi mx/\Lambda)dx. \tag{2}$$

The local Jones matrix of such a polarizer can be described as:

$$\mathbf{T} = \mathbf{R}(-\varphi)\mathbf{P}R(\varphi) = \begin{bmatrix} \cos^2\varphi & \sin\varphi\cos\varphi \\ \sin\varphi\cos\varphi & \sin^2\varphi \end{bmatrix}, \tag{3}$$

where $\mathbf{R}$ and $\mathbf{P}$ are the Jones matrices of rotation operation and a linear polarizer, respectively. As the incident field is independent of x, the far-field Fourier components can be written as:

$$\mathbf{D}_m = \mathbf{\Gamma}_m\mathbf{E}_{in}, \tag{4}$$

where the grating transfer matrix:

$$\mathbf{\Gamma}_m = \frac{1}{\Lambda}\int_0^{\Lambda} \mathbf{T}(x)\exp(-i2\pi mx/\Lambda)dx. \tag{5}$$

The grating transfer matrices solved by combining Eqs. (1), (3) and (5) for all non-zero orders are:

$$\mathbf{\Gamma}_0 = \frac{1}{2}\mathbf{I}, \tag{6}$$

$$\mathbf{\Gamma}_{\pm1} = \frac{1}{4}\begin{bmatrix} 1 & \mp i \\ \mp i & -1 \end{bmatrix}. \tag{7}$$

Optics EXPRESS

The diffraction efficiency is then calculated by the ratio of output intensity to input intensity as $\eta_m = |\mathbf{D}_m|^2 \Big/ |\mathbf{E}_{in}|^2$. For the zero and first orders, we have:

$$\eta_0 = \frac{1}{4}, \tag{8}$$

$$\eta_{\pm 1} = \frac{1}{8}(1 \mp S_3'), \tag{9}$$

where $S_3' = S_3/S_0$ is a normalized Stokes parameter. Several essential properties of a-PGs should be remarked. First, only three diffraction orders exist, which is similar to conventional PBDs. Second, the zero-order leakage not only maintains the original polarization state but also manifests a constant efficiency of 25%, no matter how the input light is polarized. Third, the sum of +1 and −1 order efficiency is also 25%, although they have a strong dependence on the input polarization state individually. In all cases, half of the incident light is absorbed by the a-PG.

3. Fabrication

In the proposed a-PGs, the dichroic dye molecules should have a linearly rotating orientation pattern. To achieve this, we usually encode such patterns with a photo-alignment layer (PAL), on which the dye-doped RMs are spin-coated and then photo-polymerized to form a solid thin film, as illustrated in Fig. 2. Several methods can provide the designed polarization field for photo-alignment, such as direct laser writing [9], analog [9,10] and digital [11,12] polarization holography, and optical polarization imprinting [13]. For higher stability, a modified Sagnac interferometer is applied in our experiments for offering a periodic polarization field, similar to the fabrication process of conventional PBDs [14]. The PAL is then coated with dye-doped RMs using a spin-coater before photopolymerization. In a-PGs, it is not necessary to manage the thickness of the self-assembled LC polymer layer to achieve half-wave retardation for high efficiency, since it works by absorption but not by retardation. Instead, the a-PG film could be thinner than conventional PBDs, especially in the long-wavelength range, if the employed dichroic dye has a high absorption coefficient and a decent dichroic ratio, which makes it an ideal polarizer at each spatial location as assumed in our paraxial analysis.

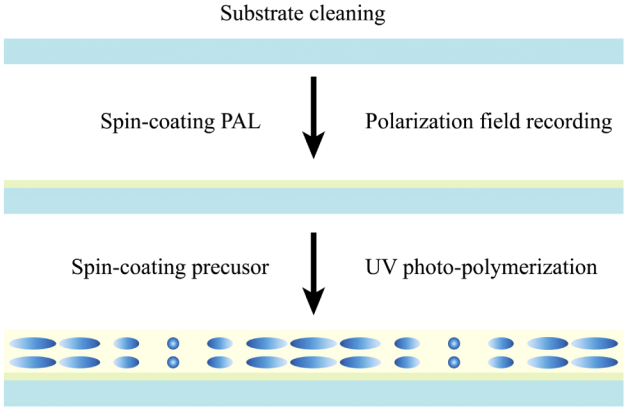

Fig. 2. Fabrication process of the a-PG, including two spin-coating and exposure steps.

In the fabrication, the solution for coating PAL is made by dissolving the photo-alignment material Brilliant Yellow (BY) in dimethylformamide (DMF) with a 0.2 wt% concentration. The precursor is a toluene-based solution, where the solute contains reactive mesogen RM257,

Optics EXPRESS

dichroic dye DDY426 (Colour Synthesis), photo-initiator Irgacure 651, and surfactant Zonyl 8857A (Dupont) mixed at 1:0.12:0.03:0.01 ratios, and the mass ratio between solute and solvent is around 1:1. The surfactant was added to help form a planar alignment at the RM-air interface after spin-coating. In the photo-alignment process, the PAL layer is exposed to a polarized light field generated by a modified Sagnac interferometer using a 457-nm laser (Cobolt Twist^{TM}) light with an intensity of 4 mW/cm^2 for 5 minutes. The sample coated with the precursor is then polymerized under a 365-nm UV lamp with a dosage of 1 mW/cm^2 for 10 minutes.

4. Results and discussion

The fabricated a-PGs exhibit ideal properties with high polarization sensitivity and low scattering. The gratings were tested with a 457-nm diode-pumped solid-state (DPSS) laser in parallel with a quarter-wave plate to control the incident polarization state, as illustrated in Fig. 3(a). Most of the output energy is shared by the zero and first different orders. A compact power meter (Thorlabs PM100D) was used to measure the intensity of each order when the quarter-wave plate was oriented at different angles. The measured diffraction efficiency of the m^{th} order is defined as

$$\eta'_m = \frac{P_m}{\sum P_m}, \tag{10}$$

where P_m is the measured power of the m^{th} diffraction order. With this definition, the Fresnel reflection loss can be avoided and an ideal a-PG should have $\eta'_0 = 50\%$ and $\eta'_{+1} + \eta'_{-1} = 50\%$ for an arbitrary input polarization state. The measured diffraction efficiency is plotted and compared with the simulation results of an ideal case in Fig. 3(b). The agreement is quite good. With this distinct polarization selectivity, the a-PGs can find promising applications for polarimetry as presented by Gori [3], and even spectropolarimetry, similar to conventional retardation-based PGs [6].

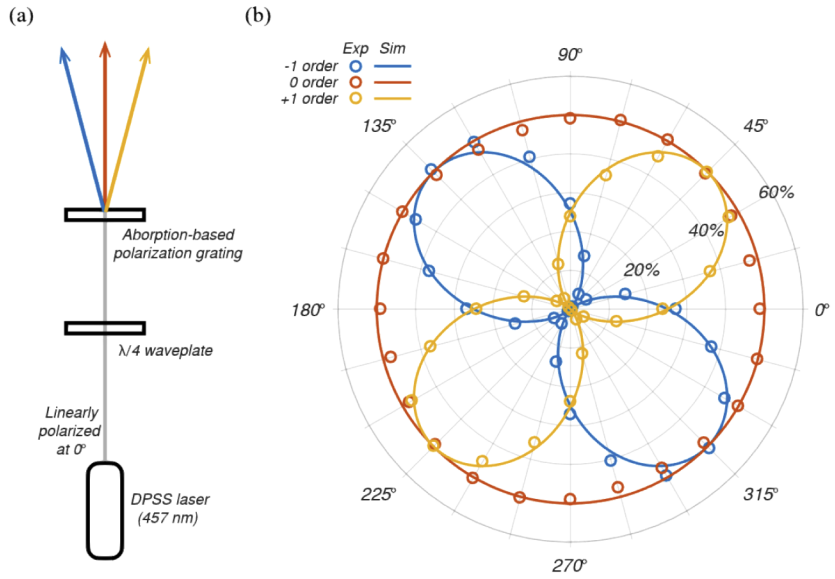

Fig. 3. Polarization response of absorption-based PGs. (a) Measurement setup including a linearly polarized laser and a rotatable quarter-wave plate to control the incident polarization. (b) Measured and calculated diffraction response to the rotation of a quarter-wave plate.

In a-PGs, the dichroic dye molecules are well aligned following the polymer networks formed by the reactive mesogens. Due to the special property of anisotropic absorption, dichroic dye

Optics EXPRESS

molecules can be considered as small-scale polarizers, although the dichroic ratio is usually in the order of 10:1. Thus, the a-PGs are also promising polarization masks that can be employed in the photopatterning of LCs, which is comparable to the photomask in the photolithography process. The difference is that photomasks control the spatial amplitude distribution of light while polarization masks determine the spatial polarization orientation. The demonstrated a-PGs can significantly simplify the fabrication process of LC-based optical components such as Pancharatnam-Berry phase optical elements (PBOEs) [15] and cholesteric LC optical elements (CLCOEs) [16], which have attracted considerable interest recently due to their numerous applications in imaging [17], lighting [18], displays [19] and even beam rider [20]. Most LC photo-patterning techniques are bulky and require complex tools such as polarization holography [14], laser-writing [9], two-photon polymerization printing [21] and even atomic force microscopy [22], which may be acceptable for research but not realistic for high-volume production. Previously, Nersisyan et al. [13] demonstrated the optical imprinting technique for PG fabrication, where a PBD is used as the polarization mask for fabricating another PBD whose period is twice as short as the master PBD. However, using PBDs, the retardation-based PGs, for optical imprinting requires a laser source and strict match between the peak efficiency of master PGs and the laser wavelength.

Here, we demonstrate the photo-patterning ability of our a-PGs, which can even work with LED light sources. As a proof of concept, we optically imprinted a PBD with an a-PG using a LED flashlight (Duracell #922241), which is a broadband, spatially and temporally incoherent light source. A photo of the optical imprint setup is shown in Fig. 4(a), where a glass substrate coated with PAL is attached to the fabricated a-PG and fixed by an optical mount (Edmund Optics #54-994). Then, the optical mount was placed on the top of the flashlight and exposed for 5 minutes. The functionality of our a-PGs as polarization masks is well evidenced by the polarized optical microscope (POM) images of the a-PG mask and optically imprinted PBD, as shown in Figs. 4(b) and 4(c), respectively. It should be noted that the proposed photopatterning process is applicable to arbitrary two-dimensional patterns, but not limited to the periodic gratings.

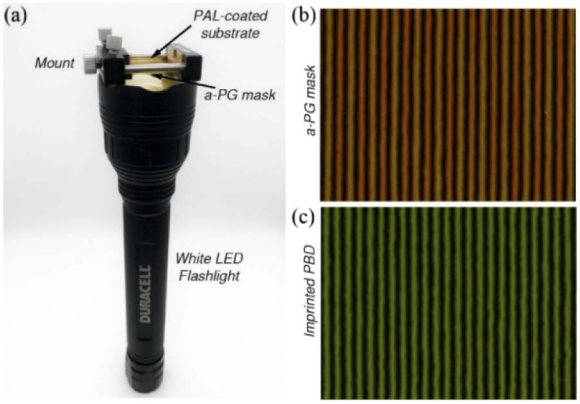

Fig. 4. Photopatterning using a-PGs as the polarization mask. (a) Contact photopatterning setup, including a flashlight as light source and an optical mount to fix the a-PG and PAL-coated substrate. POM images of the (c) a-PG mask and (d) optically imprinted PBD, where the period is around 60 μm.

5. Conclusion

We have designed and fabricated absorption-based polarization gratings based on dye-doped liquid crystal reactive mesogens. Similar to phase retardation-based polarization gratings, the absorption

Optics EXPRESS

based ones also manifest strong polarization sensitivity in their diffraction behaviors. Thanks to its absorptive nature, our a-PGs can function as efficient and LED-compatible polarization masks for high-volume photopatterning in the fabrication of emerging liquid crystal optical devices.

Funding

Air Force Office of Scientific Research (FA9550-14-1-0279).

Disclosures

The authors declare no conflicts of interest.

References

1. C. Oh and M. J. Escuti, "Achromatic diffraction from polarization gratings with high efficiency," Opt. Lett. **33**(20), 2287–2289 (2008).
2. J. Zou, T. Zhan, J. Xiong, and S. T. Wu, "Broadband wide-view Pancharatnam–Berry phase deflector," Opt. Express **28**(4), 4921–4927 (2020).
3. F. Gori, "Measuring Stokes parameters by means of a polarization grating," Opt. Lett. **24**(9), 584–586 (1999).
4. J. Tervo and J. Turunen, "Paraxial-domain diffractive elements with 100% efficiency based on polarization gratings," Opt. Lett. **25**(11), 785–786 (2000).
5. G. P. Crawford, J. N. Eakin, M. D. Radcliffe, A. Callan-Jones, and R. A. Pelcovits, "Liquid-crystal diffraction gratings using polarization holography alignment techniques," J. Appl. Phys. **98**(12), 123102 (2005).
6. M. J. Escuti, C. Oh, C. Sanchez, C. W. M. Bastiaansen, and D. J. Broer, "Simplified spectropolarimetry using reactive mesogen polarization gratings," Proc. SPIE **6302**, 630207 (2006).
7. Z. Bomzon, V. Kleiner, and E. Hasman, "Space-variant polarization state manipulation with computer-generated subwavelength metal stripe gratings," Opt. Commun. **192**(3-6), 169–181 (2001).
8. N. V. Tabiryan, S. R. Nersisyan, D. M. Steeves, and B. R. Kimball, "The promise of diffractive waveplates," Opt. Photonics News **21**(3), 40–45 (2010).
9. J. Kim, Y. Li, M. N. Miskiewicz, C. Oh, M. W. Kudenov, and M. J. Escuti, "Fabrication of ideal geometric phase holograms with arbitrary wavefronts," Optica **2**(11), 958–964 (2015).
10. D. Chen, H. Zhao, K. Yan, D. Xu, Q. Guo, L. Sun, F. Wu, V. G. Chigrinov, and H. S. Kwok, "Interference-free and single exposure to generate continuous cycloidal alignment for large-area liquid crystal devices," Opt. Express **27**(20), 29332–29339 (2019).
11. L. De Sio, D. E. Roberts, Z. Liao, S. Nersisyan, O. Uskova, L. Wickboldt, N. Tabiryan, D. M. Steeves, and B. R. Kimball, "Digital polarization holography advancing geometrical phase optics," Opt. Express **24**(16), 18297–18306 (2016).
12. Y. Li, Y. Liu, S. Li, P. Zhou, T. Zhan, Q. Chen, Y. Su, and S. T. Wu, "Single-exposure fabrication of tunable Pancharatnam-Berry devices using a dye-doped liquid crystal," Opt. Express **27**(6), 9054–9060 (2019).
13. S. R. Nersisyan, N. V. Tabiryan, D. M. Steeves, and B. R. Kimball, "Characterization of optically imprinted polarization gratings," Appl. Opt. **48**(21), 4062–4067 (2009).
14. T. Zhan, J. Xiong, Y. H. Lee, R. Chen, and S. T. Wu, "Fabrication of Pancharatnam-Berry phase optical elements with highly stable polarization holography," Opt. Express **27**(3), 2632–2642 (2019).
15. Y. H. Lee, G. Tan, T. Zhan, Y. Weng, G. Liu, F. Gou, F. Peng, N. V. Tabiryan, S. Gauza, and S. T. Wu, "Recent progress in Pancharatnam-Berry phase optical elements and the applications for virtual/augmented realities," Opt. Data Process. Storage **3**(1), 79–88 (2017).
16. J. Kobashi, H. Yoshida, and M. Ozaki, "Planar optics with patterned chiral liquid crystals," Nat. Photonics **10**(6), 389–392 (2016).
17. T. Zhan, J. Xiong, Y. H. Lee, and S. T. Wu, "Polarization-independent Pancharatnam-Berry phase lens system," Opt. Express **26**(26), 35026–35033 (2018).
18. F. Snik, M. Rodenhuis, M. J. Escuti, L. Brickson, K. Hornburg, J. Kim, C. Kievid, S. Groenhuijsen, and D. Roosegaarde, "Producing true-color rainbows with patterned multi-layer liquid-crystal polarization gratings," Opt. Mater. Express **9**(4), 1583–1589 (2019).
19. T. Zhan, Y. H. Lee, G. Tan, J. Xiong, K. Yin, F. Gou, J. Zou, N. Zhang, D. Zhao, J. Yang, S. Liu, and S. T. Wu, "Pancharatnam-Berry optical elements for head-up and near-eye displays [invited]," J. Opt. Soc. Am. B **36**(5), D52–D65 (2019).
20. Y. J. L. Chu, N. V. Tabiryan, and G. A. Swartzlander Jr., "Experimental verification of a bigrating beam rider," Phys. Rev. Lett. **123**(24), 244302 (2019).
21. Z. He, Y. H. Lee, R. Chen, D. Chanda, and S. T. Wu, "Switchable Pancharatnam-Berry microlens array with nano-imprinted liquid crystal alignment," Opt. Lett. **43**(20), 5062–5065 (2018).
22. B. S. Murray, R. A. Pelcovits, and C. Rosenblatt, "Creating arbitrary arrays of two-dimensional topological defects," Phys. Rev. E **90**(5), 052501 (2014).